# Power consumption reduction on RADAR MIMO using Lift Wavelet Transform – Orthogonal Frequency Division Multiplexing (LWT-OFDM)

RANDRIANANDRASANA Marie Emile[1], RANDRIAMITANTSOA Paul Auguste[2], RANDRIAMITANTSOA Andry Auguste[3]

[1] *Dept. of Telecommunication, Antsirabe Vankinankaratra High Education Institute, University of Antananarivo, Madagascar*
[2] *Dept. of Telecommunication, High School Polytechnic of Antananarivo, University of Antananarivo, Madagascar*
[3] *Dept. of Telecommunication, High School Polytechnic of Antananarivo, University of Antananarivo, Madagascar,*

## ABSTRACT

*The RADAR MIMO uses multiple antennas on emitter and receiver for avoiding doppler effects, improving the robustness of binary error of transmission. A multicarrier modulation like Orthogonal Frequency Division Multiplex (OFDM) is introduced. The problems of OFDM is concerned about Discret Fourier Transform (DFT) which gives Peak Average Power Ratio (PAPR) and high time processing. This article replaces the DFT by Discret Cosine Transform (DCT) and Lift Wavelet Transform (LWT).*

*This study presents the difference RADAR MIMO OFDM. We did a simulation on Matlab about the RADAR MIMO OFDM using multiple transformations like DFT, DCT and LWT and compared the results (Power Average Power Ration or PAPR, Bit Error Ratio or BER) on each methods. We present all mathematics formulas with simplified diagrams and evaluate the time complexity of each method.*

*As a result, we can deduce that time consumption for LWT is much lower than DCT and DFT. This method doesn't use exponential calculations but just addition and substraction formula. The LWT also presents a lower PAPR but has a larger BER. So, LWT-OFDM presents a good performance in reduction of power consumption on RADAR MIMO instead of classic DCT or DFT OFDM.*

**Keyword -** *RADAR, DCT, LWT, MIMO, OFDM*

## 1. INTRODUCTION

Let's a MIMO radar system colocate $N_t$ emitter antenna and $N_r$ receiver antenna. Let $S_m \in \mathbb{C}^L$, the wave on discret time which should be transmitted. Let $S = [s_1, s_2, \ldots, s_{N_t}]^T \in \mathbb{C}^{N_t \times L}$, the matrix of emitter waves where L will be the wavelength. Knowing that, the radar emits M impulsions in the interval of coherent treatment with the frequency $f_r$.

### 1.1 Target

The target catches signal coming to the emitter and sends this signal. The signal could be expressed by the equation (1) :

$$Y_{t,m} = \beta_t . exp^{j(m-1)\omega_t} a_r(\theta_t) a_t^T(\theta_t) s \tag{1}$$

Where,
$a_t(\theta_t) = [1, \ldots, e^{j(N_t-1)\pi d_t sin\theta_t}]^T$ : the vector director of the antenna emitter

$a_r(\theta_t) = [\, 1, \ldots, \; e^{j(N_r - 1)\pi d_r \sin\theta_t}\,]^T$ : the vector director of the antenna receiver.

$\theta_t$ : the target's direction of arrival

$\beta_t$ : the signal's amplitude

$\omega_t = 2\pi f_t, f_t$ : the doppler frequency of a normalized target.

## 1.2 First model of received signal

The MIMO radar will be composed by $n_T$ emitter antenna and $N_r$ receiver antenna.

A series of independent signals are transmitted in a logical manner by each transmitting element. Propagation of a signal from a transmitting element to a receiving element results in propagation through a channel with three (03) components:

- a channel of the propagation to the target
- a reflective target
- a channel reverses to the receiving probe.

The two channels will be jointly parameterized by a parametric model, from the parameter **ɣ.**

The target is considered to be specific, in other words, the physical dimensions of the target are rather small, which only turns out to be a point with the eyes of the radar. However, it is possible to consider the target as consisting of several reflecting centers.

For each transmit/receive transmission chain pair, the target response is approximated with a value to follow a random process. The equation (2) is a received signal model, due to a series of transmitted waveforms, a point target of the response vector $a$ and a parametric channel model of ɣ.

$$y = \begin{bmatrix} S(\gamma, 1) & 0 \cdots & & 0 \\ 0 & S(\gamma, 2) & \ldots \ldots & \vdots \\ \vdots & & \ddots & \\ 0 & & 0 \cdots & S(\gamma, n_R) \end{bmatrix} \begin{bmatrix} a_1 \\ a_2 \\ \vdots \\ a_{n_K} \end{bmatrix} + \begin{bmatrix} n_1 \\ n_2 \\ \vdots \\ n_{n_K} \end{bmatrix} \tag{2}$$

Let $e_k(t)$ the respective impulse response of $k$ different target.

$$e_k(t) = \sum_{r_f=1}^{R_f} m_{r_f}^{(k)} \delta\left(t - \tau_{r_f}^{(k)}\right) \tag{3}$$

Where,

$m_{r_f}^{(k)}$ and $\tau_{r_f}^{(k)}$ : the magnitudes of the response for each repair center $r_f$ and the time delay.

The transmitted waveforms $o_i(t)$ are also normalized to unity energy with energy levels defined by $p_i$ for all $i \in [1, \cdots, T]$. Each waveform is multiplied by a beamforming vector $u_i \in \mathbb{C}^{N_T X1}$ to focus on the transmitted waveforms on the radar scene.

Thus, the transmitted radar MIMO signal represents a linear combination of the totality of all beams of the transmitted and associated waves at similar energy levels. It will be expressed by the equation (4).

$$o(t) = \sum_{i=1}^{T} u_i s_i \sqrt{p_i} \tag{4}$$

Losses or pathloss in free space are expressed by $l_T^{(k)}$ and $l_R^{(k)}$ for transmitting and receiving paths relating to each k individual target of the respective radar. Since each target is at the azimuth angle $\beta_K$ relative to the transmission row, the reflected signal of the k-th target can be defined as :

$$y_k(t) = e_k(t) * \left[\beta_T^H(\beta_k) o(t) l_T^{(k)}\right], k = 1, \dots, K, \tag{5}$$

Where,

$\beta_T(\beta_K) \in \mathbb{C}^{N_T X1}$ : vector of various ranges in the direction of the target

$(*)$ : the convolution operator

$(.)^H$ : Hermitian or the complex transpose operator

When the reflected signal is received by the RADAR MIMO receiver, the received signal is expressed as the equation (6) :

$$z_r(t) = \sum_{k=1}^{K}\sum_{i=1}^{T} \alpha_{ri}^{(k)} [e_k(t) * o_i(t)]\sqrt{p_i} + \sum_{e=1}^{C_x}\sum_{i=1}^{T} \mu_{ri}^{(e)} [e_e(t) * o_i(t)]\sqrt{p_i} + v_r^H \eta(t) \tag{6}$$

Where,

$\beta_R(\theta_k) \in \mathbb{C}^{N_R X1}$ : the vector director of various ranges of reception antenna of the azimuth direction

$\theta_k, \alpha_{ri}^{(k)} = l_R^{(k)} v_r^H \beta_R(\theta_k) \beta_T^H(\beta_k) y_k l_T^{(k)}$ : reflexion coefficient

$e = 1, \dots, c_g$ : source of clutter

The coefficients of periodic reflection and complexes of "clutter" $\mu_{ri}^{(e)}$ is defined by $\alpha_{ri}^{(k)}$ for the target radar with $\mu_{ri}^{(e)} = l_R^{(k)} v_r^H \beta_R(\tilde{\theta}_e) \beta_T^H(\tilde{\beta}_e) y_k l_T^{(k)}$ .

Note that, $\mu_{ri}^{(e)}, l_R^{(k)}$ and $l_T^{(k)}$ define the pathloss coefficients corresponding to each source and "clutter" for the transmission and receiving paths, respectively.

The coefficient $\tilde{\beta}_e$ and $\tilde{\theta}_e$ indicates the azimuths at which each source of "clutter" is produced relative to the transmission and receiving ranges, respectively.

### 1.3 Second model of received signal

In this second theory, Uniform Linear Antenna (ULA) uses a vector director to beam the signal in a specific direction. The signal to be transmitted is defined by the equation (7) :

$$x(m) = [x_1(m) \; x_2(m) \dots x_{n_T}(m)] \tag{7}$$

$x_n(m)$ : the bandbase signal of the m-ith emission element at the time index m.

The target with (his emplacement $\theta_k$ ) receives the signal expressed by :

$$r_k(m) = \sum_{n=1}^{n_T} e^{-j(n-1)\pi \sin \theta_k} x_n(m), with, k = 1, 2, \dots K \tag{8}$$

$$r_k(m) = a^H(\theta_k)x(m) \tag{9}$$

Where : $a(\theta_k)$ is the vector director defined by :

$$a(\theta_k) = [\,1 \quad e^{j\pi sin\theta_k} \quad e^{j2\pi sin\theta_k} \ldots \ldots \ldots e^{j(n_T-1)\pi sin\theta_k}\,] \tag{10}$$

## 2. MATERIAL AND METHODS
### 2.1 Offset of Quadrature Amplitude Modulation (OQAM) on advanced modulation

The techniques of OQAM is based on two principles :

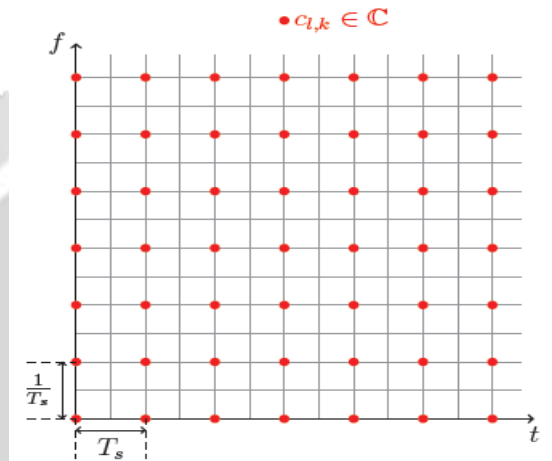- On the emitter, the OQAM preprocessing

- On the receiver, the OQAM postprocessing



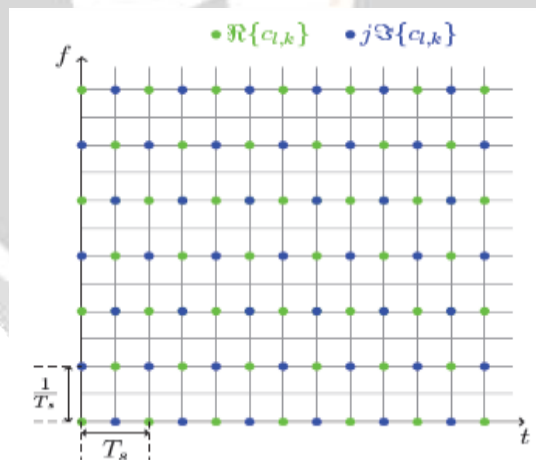**Fig. 1.** : *Time latency with QAM*



**Fig. 2.** *Time latency with O-QAM*

The first operation in the pre-processing block is the complex/real conversion. Indeed, instead of sending complex symbols (QAM symbols). The fig. 1 and 2 show the difference between time latency using QAM processing and OQAM processing with advanced modulation. The constant k and l represent the temporal index and the frequency index, respectively.

The objectives of OQAM are:
- Two symbols on the same carrier must be successively real and purely imaginary.
- In addition, the adjacent symbols between the two under carrier must also be successively real and purely imaginary.

Let $C_{l,k}$ the complex symbols that after OQAM modulation will become real symbols $a_{l,k}$ expressed by the equation (11). Recall that k is the temporal index and the frequent index.

$$a_{l,k} = \begin{cases} Real(C_{l,k}) \; si \; l \; pair \; et \; k \; pair \\ Imag(C_{l,k}) \; si \; l \; impair \; et \; k \; pair \\ Imag(C_{l,k}) \; si \; l \; pair \; et \; k \; impair \\ Real(C_{l,k}) \; si \; l \; impair \; et \; k \; impair \end{cases}$$

(11)

The second operation of the OQAM pre-processing block is a multiplication by: $\theta_{l,k} = j^{l+k}$.

The symbols at the exit of the OQAM pre-processing block will modulate the carrie and which notes $X_{l,k}$ like on expression :

$$X_{l,k}(t) = \sum_{k=-\infty}^{+\infty} \theta_{l,k}.a_{l,k}.\delta(t - k\frac{T_s}{2})$$

(12)

Where,

$\delta(t)$ : impulsion of Dirac

The first operation of the OQAM post-processing block is multiplication by $\theta^*_{l,k}$ which is a conjugate complex of $\theta_{l,k}$. Then, there is a real/complex conversion. Indeed, two real symbols successively on a carrier form a complex symbol. The equation (13) gives the expression of complex symbols on the carrier l after OQAM post-processing.

$$C_{l,k} = \begin{cases} a_{l,k} + a_{l,k+1} \; si \; l \; pair \; et \; k \; pair \\ a_{l,k+1} + a_{l,k} \; si \; l \; impair \; et \; k \; pair \\ a_{l,k-1} + a_{l,k} \; si \; l \; pair \; et \; k \; impair \\ a_{l,k} + a_{l,k-1} \; si \; l \; impair \; et \; k \; impair \end{cases}$$

(13)

## 2.2 DFT-OFDM

By default the classic trasform used with OFDM is the IDFT in the transmitter and DFT in the receiver. The IDFT could be expressed in the equation (14).

$$x(t) = \sum_{n=0}^{N-1} \frac{1}{\sqrt{N}} exp^{(j2\pi\frac{nt}{N})} s_{i,n}(t).g(t - kT)$$

(14)

Where,
$s_n$ : Symbol carried by the n-th subcarrier
g  : Rectangular function with period T
$N$ : Number of subcarriers of IDFT

To recover the signal, the DFT process should be done as expressed in the equation (15)

$$s_{i,n}(k) = \frac{1}{N} \sum_{k=0}^{N-1} x(k).e^{j\frac{2\pi}{N}k.n}$$

(15)

**2.3 DCT-OFDM**

The IDFT on OFDM could be replace by IDCT which could be expressed by the equation (16).

$$x(t) = \sum_{n=0}^{N-1} \beta_n . \cos(\frac{\pi(2t-1)(n-1)}{2.N}) s_{i,n}(t) . g(t-kT)$$

(16)

Where,

$s_n$ : Symbol carried by the n-th subcarrier
$g$  : Rectangular function with period T
$N$ : Number of subcarriers of IDFT
And

$$\beta_n = \begin{cases} \frac{1}{\sqrt{2}} \; if \; n = 0 \\ 1 \; if \; 2 \leq n \leq N-1 \end{cases}$$

(17)

To recover the signal, the DCT process should be done as expressed in the equation (18)

$$s_{i,n}(k) = \sqrt{\frac{2}{N}} . \sum_{k=0}^{N-1} x(k) . \beta_k . \cos\left(\frac{\pi . (2n-1) . (k-1)}{2N}\right)$$

(18)

**2.4 LWT-OFDM**

The IDFT on OFDM could be also replaced by ILWT. The ILWT is defined by a sequence $\{Y(z)\}$, and can be given by the equation (19).

$$y_{ILWT}[t] = \sum_{q=0}^{Q-1} \sum_{n=0}^{N-1} (s_{i,n}(t))^q . (2)^{\frac{q}{2}} . \psi(2^q . t - n)$$

(19)

To recover the signal, the LWT process should be done as expressed in the equation (20).

$$s_{LWT}^q(z) = \sum_{k=0}^{N-1} (x(k)) . 2^{\frac{z}{2}} \psi(2^z . k - q); \quad z = 0,1,2,\dots,N-1 \; and \; q = 0,1,2,\dots,N-1$$

(20)

An alternative method for constructing the biorthogonal wavelet transform, the lifting scheme in fig. 3 and fig. 4, has some advantages over the classical standard wavelet transform which are given below.

- It is a spatial domain method,
- It is easy to use for implementation,
- It allows the use of quicker and in-place computations,
- It allows the use of nonlinear, adaptable, disorderedly sampled and integer to integer wavelet transforms,

Another advantage of the lifting scheme is that the LWT and the reverse-LWT shown in fig. 3 and  fig. 4 are completely symmetrical to each other. This ensures that LWT can be applied easily.

Filters and subsampling are used in traditional wavelet transform processes. The lifting method was developed by Sweldens in 1992 to reduce the complex mathematical operations used in filtering. The lifting method is the simplest and most efficient method for wavelet transformation.

In the lifting method, the signal is divided into odd and even samples. Instead of filters, Spit Predit and Update processes are applied. Complex calculations are not required for these operations as in traditional methods.

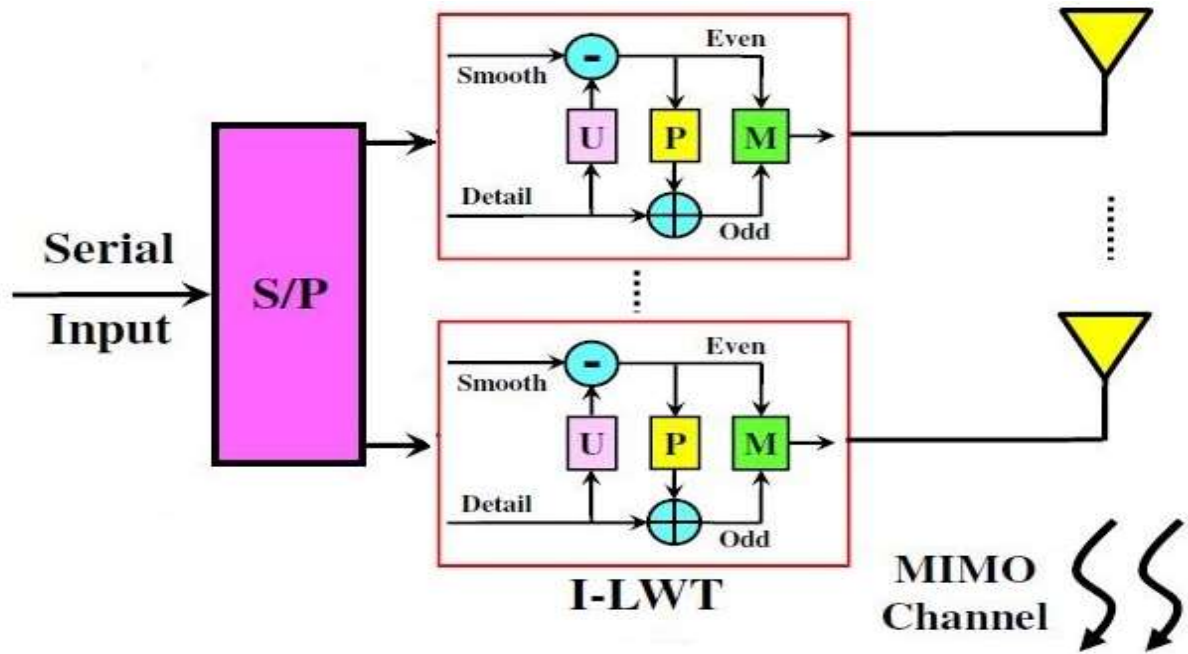In the figure, U means *Update*, P means *Prediction*, S means *Spit* and M means *Merge*.



**Fig. 3.** *Fast computation ILWT*

The original X[k] signal is primarily separated into odd and even components, as in the equations (21) and (22).

$$X_{odd}[k] = X[2k + 1] \tag{21}$$

$$X_{even}[k] = X[2k] \tag{22}$$

There is a strong correlation between these two examples. In the predict step, odd samples are tried to be obtained approximately by making use of even samples. The second part, Predict, preserves the high frequency components by eliminating the low frequency components of the signal. In the prediction process, the subset $X_{odd}[k]$ is predicted over the subset $X_{even}[k]$ using the prediction operator P(.). The detail information of the X[k] signal is obtained as in equation (23) by taking the difference between the subset $X_{odd}[k]$ and the predicted P($X_{even}[k]$). The P(.) Prediction operator is a linear combination of a single neighboring subset.

$$P(X_{even}[k]) = \sum_i (p_i \cdot X_{even}[k + i]) \tag{23}$$

Here, $p_i$ are the prediction coefficients. This step acts as a high pass filter and the high frequency components (d[k]) that give the detail part of the obtained signal.

$$d[k] = X_{odd}[k] - P(X_{even}[k]) \tag{24}$$

After calculating the prediction $p_i$,

$$d[k] = d[2y + 1] = \begin{cases} X[2y + 1] - \dfrac{X[2y] + X[2y + 2]}{2} & Normal \\ X[2y + 1] - X[2y] & Odd\ end \end{cases}$$
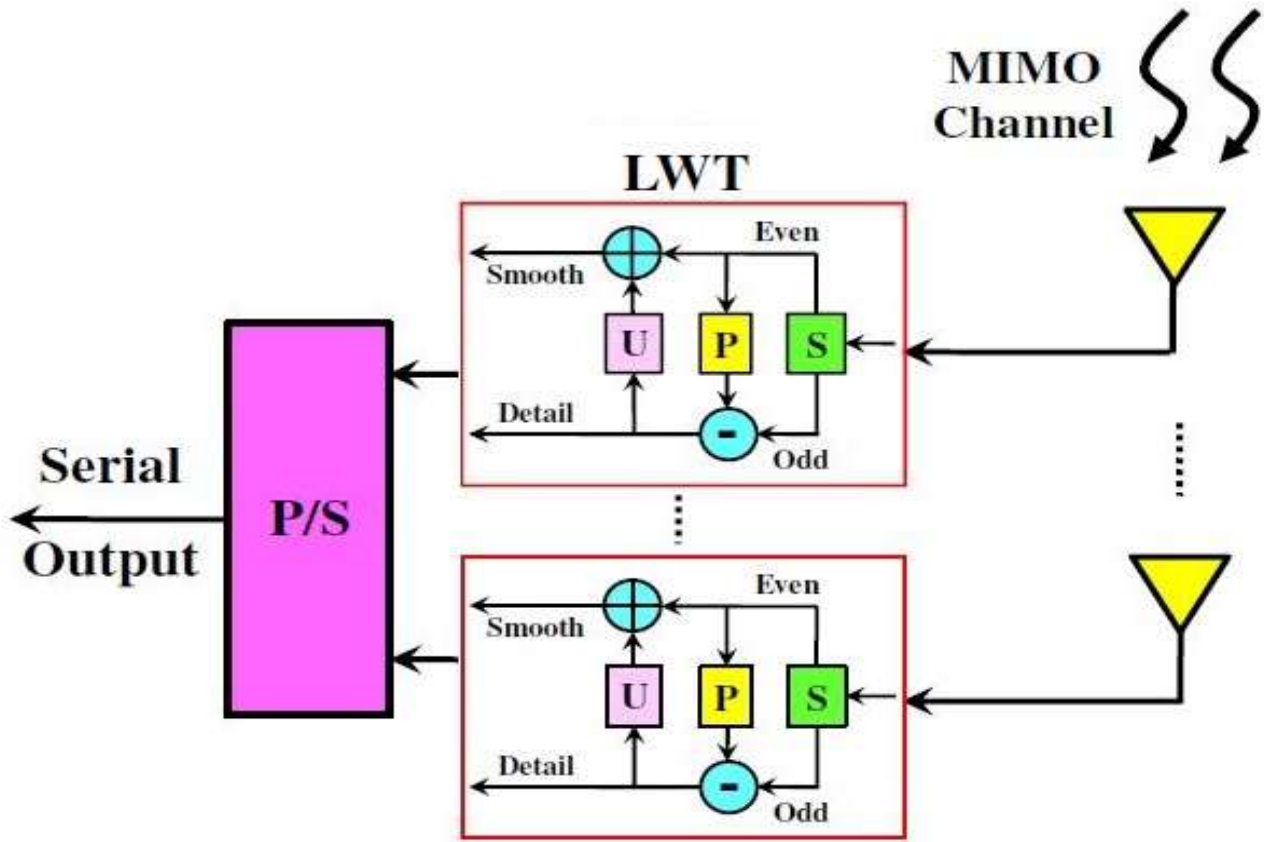
(25)



**Fig. 4.** *Fast computation LWT*

In the update step, the samples are scaled to fix and then added with even samples to provide low pass filtered values for transformation. In the third part, update, the even components are updated by using the detailed signal to reduce the frequency aliasing effect.

In the update process, the approximate information about the signal is obtained as a result of collecting the detailed information entering the U(.) Update operator with the subset $X_{even}[k]]$. The U(.) Update operator is a linear combination of neighboring d[k] values. The formula for the U(.) Update operator is specified in equation (26).

$$U(d[k]) = \sum_i (u_i d[k + i])$$

(26)

Here, $u_i$ are the updating coefficients. In the update process, the approximate value of the obtained signal by passing the signal through a low pass filter is obtained by updating the linear combination of the d[k] prediction difference as in the equation (27). These examples contain low frequency components that give approximate information (s[k]) about the signal.

$$s[k] = X_{even}[k] + U(d[k])$$

(27)

After calculating the prediction $u_i$,

$$s[k] = s[2y] = \begin{cases} X[2y] + \dfrac{V[2y+1]+1}{2} & Normal \\ X[2y] + \dfrac{X[2y-1] - X[2y]+1}{2} & Even\ end \end{cases}$$

(28)

Inverse transformation is obtained by applying the exact opposite operations used in the conversion to the obtained d[k] and s[k] signals. Inverse Lifting wavelet transformation is given in fig. 3 in I-LWT block in detail.

$$X_{odd}[k] = d[k] + P(X_{even}[k])$$

(29)

$$X_{even}[k] = s[k] - U(d[k])$$

(30)

After the inverse transformation process, as given in equation (31), the original signal is obtained by combining the odd index and even index samples with the MRG combination operator.

$$X[k] = MRG\{X_{odd}[k], X_{even}[k]\}$$

(31)

The equations (24) and (27) could be performed using the matrix form expressed in the equation (32).

$$\begin{bmatrix} d[k] \\ s[k] \end{bmatrix} = \begin{bmatrix} 1 & -P(.) \\ U(.) & 1 - P(.)U(.) \end{bmatrix} \cdot \begin{bmatrix} X_{odd}[k] \\ X_{even}[k] \end{bmatrix} = A. \begin{bmatrix} X_{odd}[k] \\ X_{even}[k] \end{bmatrix}$$

(32)

With,

$$A = \begin{bmatrix} 1 & -P(.) \\ U(.) & 1 - P(.)U(.) \end{bmatrix}$$

(33)

For the ILWT, the equations (29) and (30) could be simplified using the matrix form expressed in the equation (34) :

$$\begin{bmatrix} X_{odd}[k] \\ X_{even}[k] \end{bmatrix} = \begin{bmatrix} 1 - P(.)U(.) & P(.) \\ -U(.) & 1 \end{bmatrix} \cdot \begin{bmatrix} d[k] \\ s[k] \end{bmatrix} = A^{-1}. \begin{bmatrix} d[k] \\ s[k] \end{bmatrix} = A.A. \begin{bmatrix} d[k] \\ s[k] \end{bmatrix}$$

(34)

With,

$$A^{-1} = A.A = \begin{bmatrix} 1 - P(.)U(.) & P(.) \\ -U(.) & 1 \end{bmatrix}$$

(35)

## 2.5 Multiple Transform of OFDM-OQAM

In MIMO radar system with M transmitter antennas and N receiver antennas, the transmitters are placed parallel to the axis of the abscesses are its antennas are spaced a distance dt, as the coordination of the same meter antenna is expressed by the equation (36).

$$E_m = E_0 + m.d_t.x.$$

(36)

Where, m= 0,… ,M-1 and $E_0 = [x_{t,0}, y_{t,0}, z_{t,0}]^T$

the first transmitter is located in the center O(0,0,0) and et $x = [1,0,0]^T$ is the unitary vector on the axis of x. Similar, the receivers are parallel to the order axis, they are spaced a distance $d_r$, n-ith receiver antenna are located on coordinate by the equation (37) :

$$R_n = R_0 + n.d_r.y,$$

(37)

Where, $R_0 = [x_{r,0}, y_{r,0}, z_{r,0}]^T$ and $y = [0,1,0]^T$

Each element in a transmitter system transmits a signal modulated in OFDM at an initial carrier frequency $f_0$. The base band OFDM signal consists of N sub-carrier frequencies with a uniformly spaced frequency $\Delta f$; the total bandwidth is expressed by the equation (38).

$$B\omega = N.\Delta f \tag{38}$$

The n-ith sub-carrier is modulated with a K-ith code sequence and it will be formulated by the equation (39) and the code should respect the orthogonal waveform condition :

$$c_{n,p} = \left[b_{n,p}^{(0)}, \dots, b_{n,p}^{(K-1)}\right]^T \tag{38}$$

Where, $c_{n,p}^H c_{n,p} = \begin{cases} 1, & p = p' \\ 0, & p \neq p' \end{cases}$

So, $c_n = \left[c_{n,0}, \dots, c_{n,P-1}\right] \in C^{K \times P}$ and the expression could be rewrited like :

$$c_n^H c_n = I_n$$

The bit length $t_b$ respects the orthogonality condition $t_b.\Delta f = 1$. The m-ith impulsion on the baseband OFDM could be expressed by the equation (40).

$$u_m(t) = \sum_{n=0}^{N-1} \sum_{k=0}^{K-1} b_{n,m}^{(k)} exp^{\{j2\pi t \Delta f(t-(k+1))t_c\}} rect(\frac{t - kt_s}{t_s} - \frac{1}{2}) \tag{40}$$

With,

$t_s = t_b - t_c$ : symbol duration
$t_c = \propto t_b$ : cyclic prefix duration
m = 0,…,P-1
$rect(t) = \begin{cases} 1, & \frac{-1}{2} \leq t < \frac{1}{2} \\ 0, & ailleurs \end{cases}$ : rectangular signal

The baseband signal $u_m(t)$ is modulated with an initial carrier frequency $f_0$ for transmitting.
A target set is composed of the scattered ideal points I. The coordinate of i-th dispersed point is expressed by :

$$D_i = [x_i, y_i, z_t]^T \tag{41}$$

The amplitude of the relative dispersion is $\sigma_i$, which is a constant within an OFDM pulse width and for multiple transmitter/receiver channels.
The target velocity is fully estimated and compensated after pre-processing. The Doppler effect is negligible in all echo models as expressed by the equation (42):

$$t = \tau_{min} + kt_s + t_c + t_0, \tag{42}$$

With,
$\tau_{min}$ : being the beginning of a sample
$t_0 \in [0, t_b]$ : initial time
The time interval of a (p,q)-th transmit/receive chain and i-th scatter is expressed by the equation (43).

$$\tau_{p,q}^{(i)} = \frac{(\|D_i - t_p\| + \|R_q - S_i\|)}{C} - \tau_{min} \tag{43}$$

Where,
c : the speed of light
The echo after the downlink is expressed by the equation (44).

$$s_q^{(k)}(t_0) = \sum_{p=0}^{P-1} \sum_{i=1}^{I} \sigma_i exp^{(-j2\pi f_0 \tau_{p,q}^{(i)})} \sum_{n=0}^{N-1} exp^{\{i2\pi \Delta f(t_0 - \tau_{p,q}^{(i)})\}} \sum_{k'=0}^{K-1} b_{n,p}^{(k')}$$

$$rect\left(\frac{(k-k')t_s + t_c + t_0 - \tau_{p,q}^{(i)}}{t_s} - \frac{1}{2}\right) + \vartheta_q^{(k)}(t_0)$$

(44)

Where,

$\vartheta_q^{(k)}(t_0)$ : the noise

and $rect\left(\frac{(k-k')t_s + t_c + t_0 - \tau_{p,q}^{(i)}}{t_s} - \frac{1}{2}\right) = \delta(k-k')$ ; $\delta(.)$ is an impulse function.

For the following, the processing methods will be described.
For q-th element received, and for k-th OFDM bit, the DFT calculation follows the sample index at a fast time. The echo in a frequency domain is written by the equation (45).

$$x_{n,q}^{(k)} = \frac{1}{N}\sum_{n=0}^{N-1} exp^{\left(j2\pi\frac{nl}{N}\right)} s_{lq}^{(k)} = \sum_{i=0}^{I} \sigma_i exp^{\{-j2\pi(n\Delta f + f_0)\tau_{p,q}^{(i)}\}} \sum_{p=0}^{P-1} b_{n,p}^{(k)} + V_{lq}^{(k)}$$

(45)

Where,

$x_{n,q}^{(k)}$: the n-th point results of the DFT and the echo in a frequency domain with n-th subcarrier

$V_{lq}^{(k)}$: the noise

N sub-carriers are separated without inter-carrier interference but the echoes received in P transmitting antennas are multiplexed and named serial to parallel.

To separate the transmitter and decode the sub-carriers, each sub-carrier is indexed n, we stack the DFT results of the K bits in a column vector :

$$s_{n,q} = \left[S_{n,q}^{(0)}, ..., S_{n,q}^{(K-1)}\right]^T$$

(46)

Let,

$$s_{n,q} = C_n E_{n,q}\sigma + v_{n,q} \in \mathbb{C}^{K\times 1}$$

(47)

Where,

$C_n \in \mathbb{C}^{K\times P}$ and $E_{n,q}$ : complex matrix with dimension $P \times I$

$\varepsilon_{n,p,q}^{(i)} = exp^{\{-j2\pi(n\Delta f + f_0)\tau_{p,q}^{(i)}\}}$ : element of matrix $C_n$ and the response of i-th disperser to n-th subcarrier for (p,q)-the transmitter/receiver chain.

$\sigma = [\sigma_1, ..., \sigma_i]^T$: dispersion coefficient

$v_{n,q} = \left[V_{n,q}^{(0)}, ..., V_{n,q}^{(K-1)}\right]^T \in \mathbb{C}^{K\times 1}$ : vector noise

Let,

$$R_{n,q} = \left[r_{n,0,q}, ..., r_{n,P-1,q}\right]^T \in \mathbb{C}^{K\times 1}$$

(48)

$$R_{n,q} = C_n^H x_{n,q} = E_{n,q}\sigma + v'_{n,q}$$

(49)

Where,

$r_{n,p,q}$ : modulated echo

$v'_{n,q}$ : the noise vectors modified without power change

For each OFDM subcarrier, each transmitter/receiver pair :

$$\varepsilon_{n,p,q}^{(0)} = exp^{\{j2\pi(n\Delta f + f_0)\tau_{p,q}^{(0)}\}},$$

$$\tau_{p,q}^{(0)} = \frac{\|o - Z_p\| \|W_q - o\|}{C} - \tau_{min}$$

$$(50)$$

$r_{n,p,q}$ is multiplied by $\varepsilon_{n,p,q}^{(0)}$ for a compensated initial phase

$$h_{n,p,q} = \varepsilon_{n,p,q}^{(0)} r_{n,p,q} = \sum_{i=1}^{I} exp^{\{j2\pi(n\Delta f + f_0)(\tau_{p,q}^{(0)} - \tau_{p,q}^{(i)})\}} \sigma_i + \tilde{v}_{n,p,q}$$

$$(51)$$

$\tilde{v}_{n,p,q}$ is the noise after compensation. Then,

$$\tau_{p,q}^{(0)} - \tau_{p,q}^{(i)} = \frac{\|o - Z_p\| + \|W_q - o\| - \|h_i - Z_p\| - \|W_q - h_i\|}{C}$$

$$(52)$$

With,

$Z_p$ the p-th transmitter et $W_q$ the q-th receiver.

If $\tilde{\sigma}_i = \sigma_i exp\{j2\pi\frac{(-2u_i + \mu_i)}{\lambda}\}$ designates the modulated dispersion amplitude phase, which is a constant for a transmitter/receiver chain.

$$\begin{cases} \Delta u = \frac{c}{2N\Delta f} \\ \Delta \tilde{x} = \frac{cd_0}{P f_0 d_t} \\ \Delta \tilde{y} = \frac{cd_0}{Q f_0 d_r} \end{cases}$$

$$(53)$$

The equation (31) expresses the resolution of the radial distance and the section respectively, with $\lambda_0 = \frac{c}{f_0}$ being the wavelength of the system. $Pd_t$ and $Qd_r$ is the distances between the transmitters, and $QD_r$ is the distance between the receivers.

$$u_i = \bar{h}_i^T d_0 \qquad (54)$$

$$\bar{h}_i = h_i - o \qquad (55)$$

$$(\tilde{x}_i, \tilde{y}_i, \tilde{z}_i)^T = \bar{h}_i - u_i d_0 \qquad (56)$$

$$\mu_i = (\bar{h}_i - u_i d_0)^T (Z_0 + W_0) \qquad (57)$$

With,

$u_i$ : the radial distance

The signal received is therefore expressed by the equation (58).

$$h_{n,p,q} = \varepsilon_{n,p,q}^{(0)} r_{n,p,q} = \sum_{i=1}^{I} \tilde{\sigma}_i . exp^{\{j\pi\omega_{1,i} + jP\omega_{2,i} + jQ\omega_{3,i}\}} + \tilde{v}_{n,p,q}$$

$$(58)$$

$$\text{With,} \begin{cases} \omega_{1,i} = \dfrac{-2\pi\lambda_i}{N\,\Delta u} \\ \omega_{2,i} = \dfrac{2\pi\ell_i}{P\,\Delta\ell} \\ \omega_{3,i} = \dfrac{2\pi\hat{y}_i}{Q\,\Delta\hat{y}} \end{cases}$$

After the OFDM theory on transmitter and receiver signal, the OQAM processing could also be applied to it.

On the OQAM-OFDM, the modulated signal will be expressed by the equation (59).

$$x(t) = \sum_{n=0}^{N-1} \frac{1}{\sqrt{N}} exp^{\left(j2\pi\frac{tn}{N}\right)} s_n = V.S$$

(59)

$N$ : Number of subcarriers of IDFT
V : Columns of IDFT
S : vector of symbol O-QAM
$s_n$ : symbol OQAM carried by the n-th subcarrier expressed by the equation (60)

$$s_n(t) = \theta_{l,k}.a_{l,k}.\delta(t - k\frac{T_s}{2})$$

The classic OFDM use IDFT and DFT. In this article we propose to comparte this IDFT by Inverse Multiple Transform noted by IMT (IDCT, IDFT and ILWT) on transmitter and DFT by Multiple Transform (DCT, DFT and LWT). All diagrams will be resume by the next figure 5 and 6.
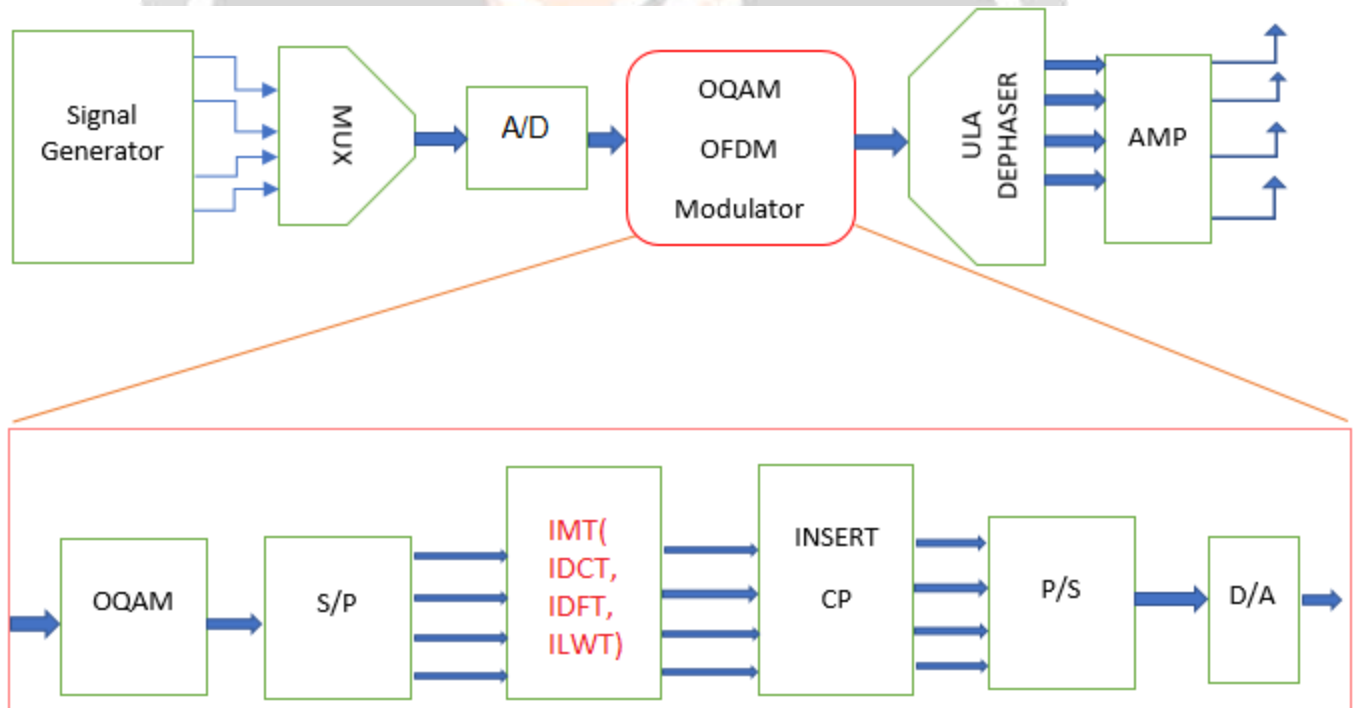


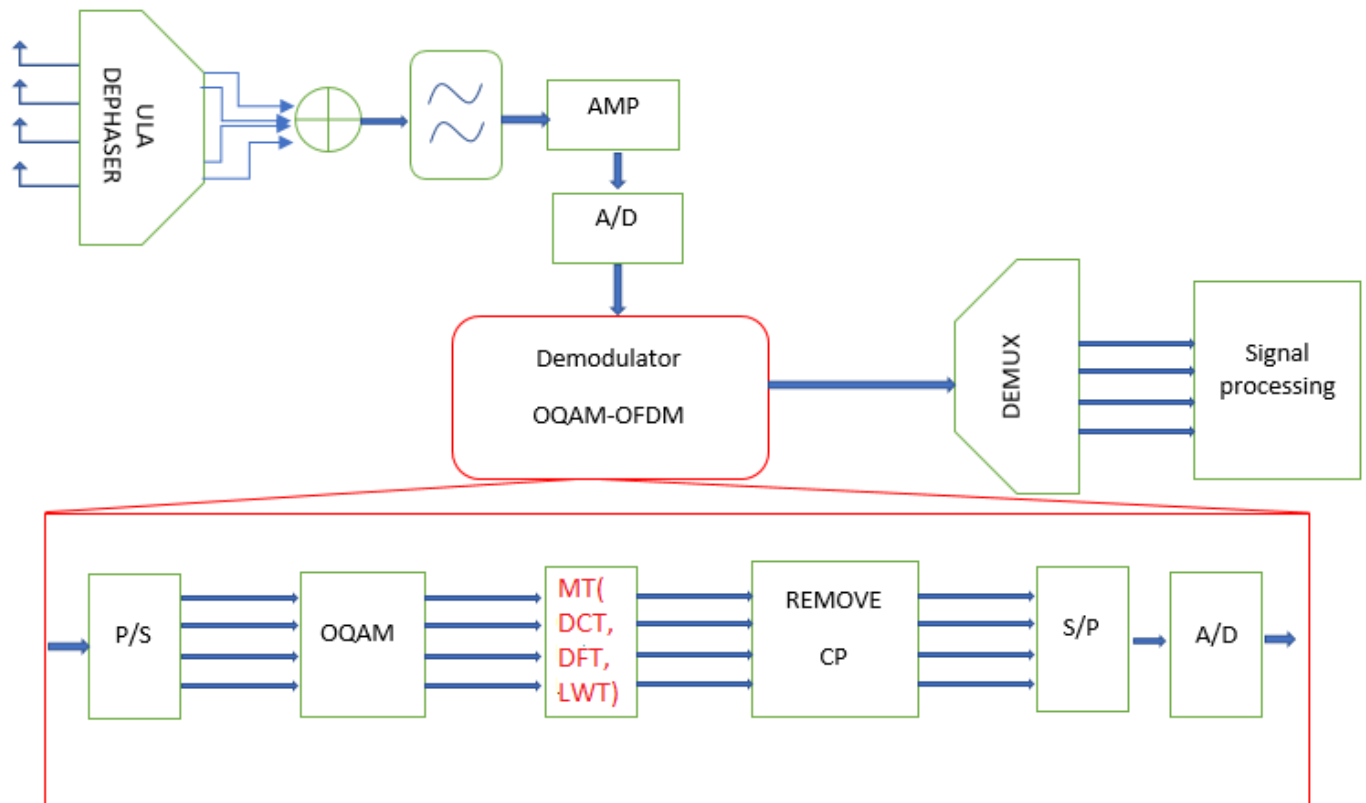**Fig. 5.** *OFDM OQAM transmitter for MIMO Radar*

**Fig. 6.** *OFDM OQAM receiver for MIMO Radar*

The operators in the fig. 5 and fig. 6 are :

- Signal generator : generate binary data to be sent
- MUX : Multiplexing the multiple signals generated to be sent on one channel
- A/D : Analog to digital
- S/P : Serial to Parallel
- IMT : IDCT or IDFT or ILWT
- CP : Clipping
- ULA dehaser : equation (10)
- AMP : Amplifier
- D/A : Digital to Analog
- P/S : Parallel to Serial
- FFT : Fast Fourier Transform

## 3. RESULTS AND DISCUSSIONS
### 3.1 Power Spectrum Density

The three fig. 7,8,9 give the spectrum of modulated signal using Inverse Multiple Transform with OFDM. The classic IDFT shows that it has more spectrum efficient than the IDCT and ILWT. But, the difference it's not so big indeed between IDFT-OFDM and IDCT-OFDM. Due to interpolation of ILWT, The ILWT-OFDM is not so orthogonal. So the interference between the multi-carriers should be large. Even IDCT has this problem.

The power spectrum analyzer is obtained after the full schema bloc of OFDM on fig.5 by changing IMT respectively to IDFT, IDCT and ILWT.
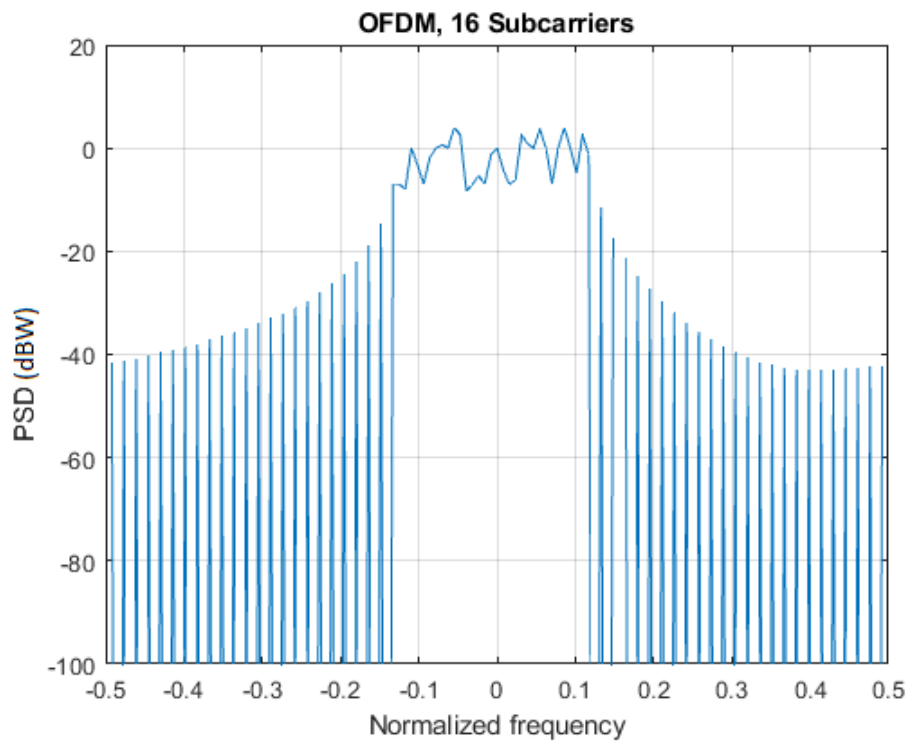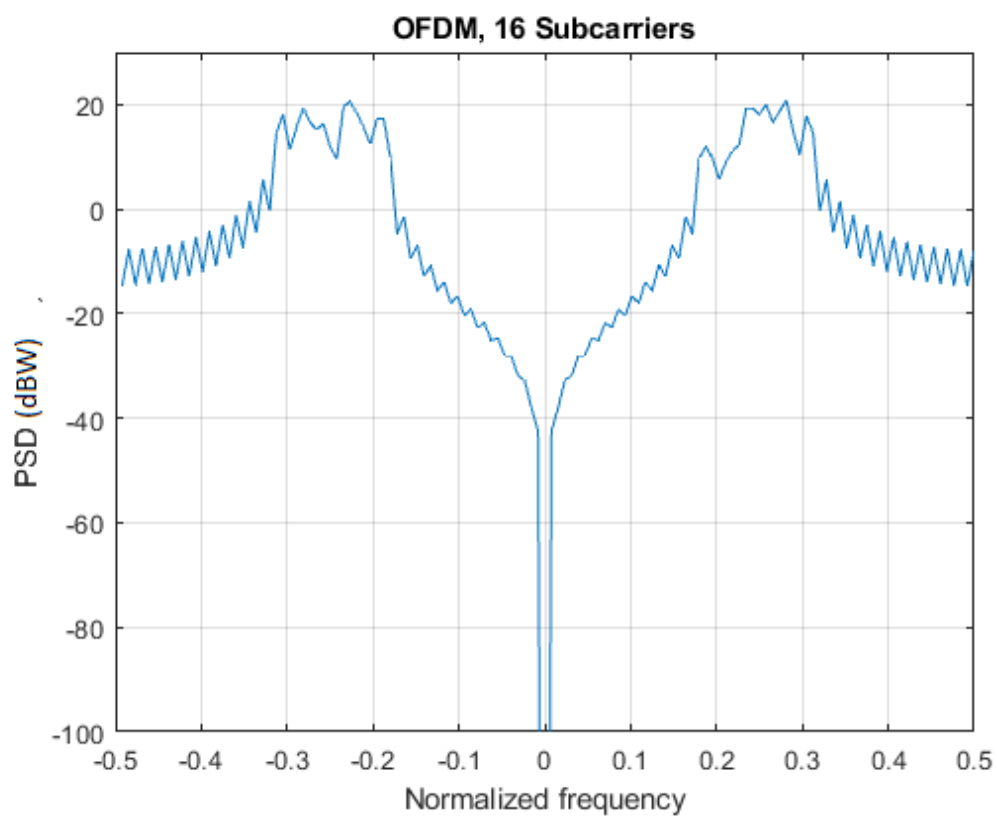
**Fig. 7.** *Power Density Spectrum of OFDM with IDFT*



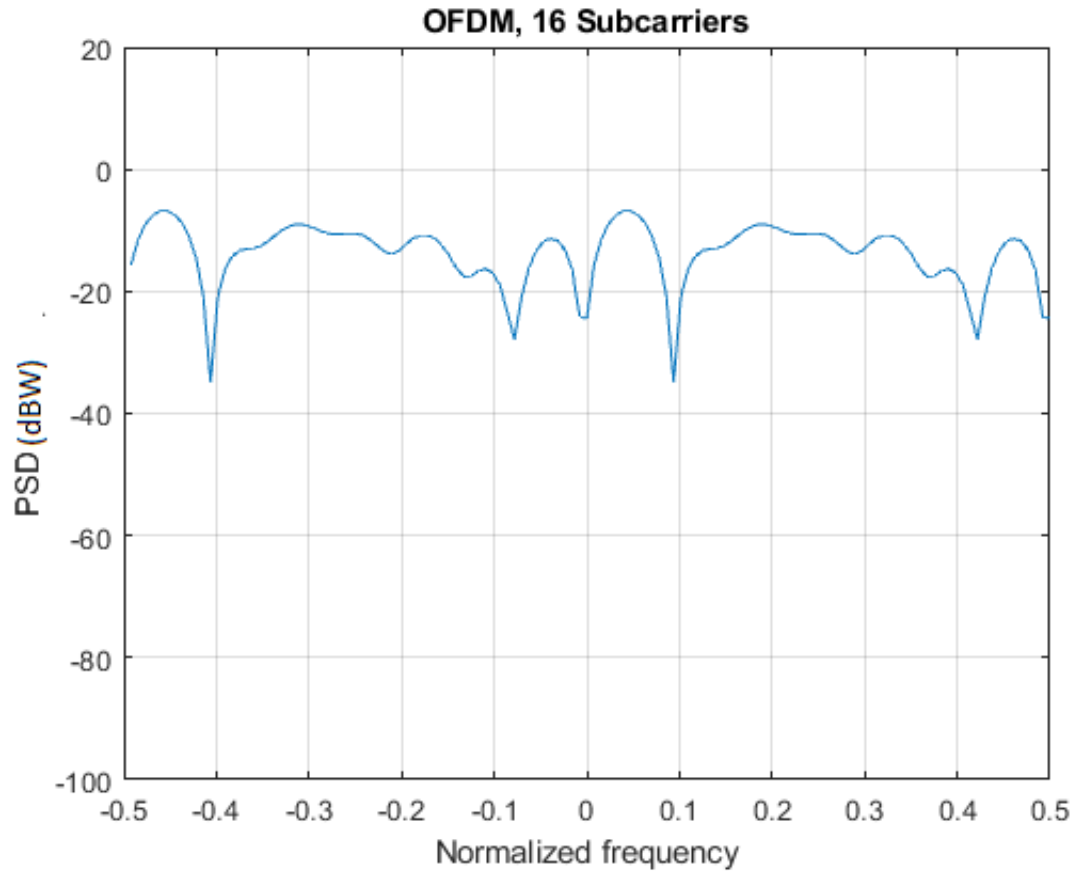**Fig. 8.** *Power Density Spectrum of OFDM with IDCT*

**Fig. 9.** *Power Density Spectrum of OFDM with ILWT*

We don't vary the number of sub-carries. When the sub-carries are big, the two modulations could give a same performance. So, this result with 16 sub-carries gives us the worst case for spectrum analyzer.

### 3.2 Modulated signal

The fig 10,11,12 is a representation of modulated signal of OFDM using respectively IDFT, IDCT and ILWT. The fig.12 could be interpret as the advantage of the ILWT. This transform doesn't present of a big variation on the signal. The transformation combined the detaills information and the smooth information to having a modulated signal like in fig 12.

About the two figure based on exponential formula of IDFT and IDCT, the modulated signal presents a big variation on amplitude. It's not very good for the amplifier. Energy will be lost as thermal dissipation and the two schema has a big power consumption than the ILWT.
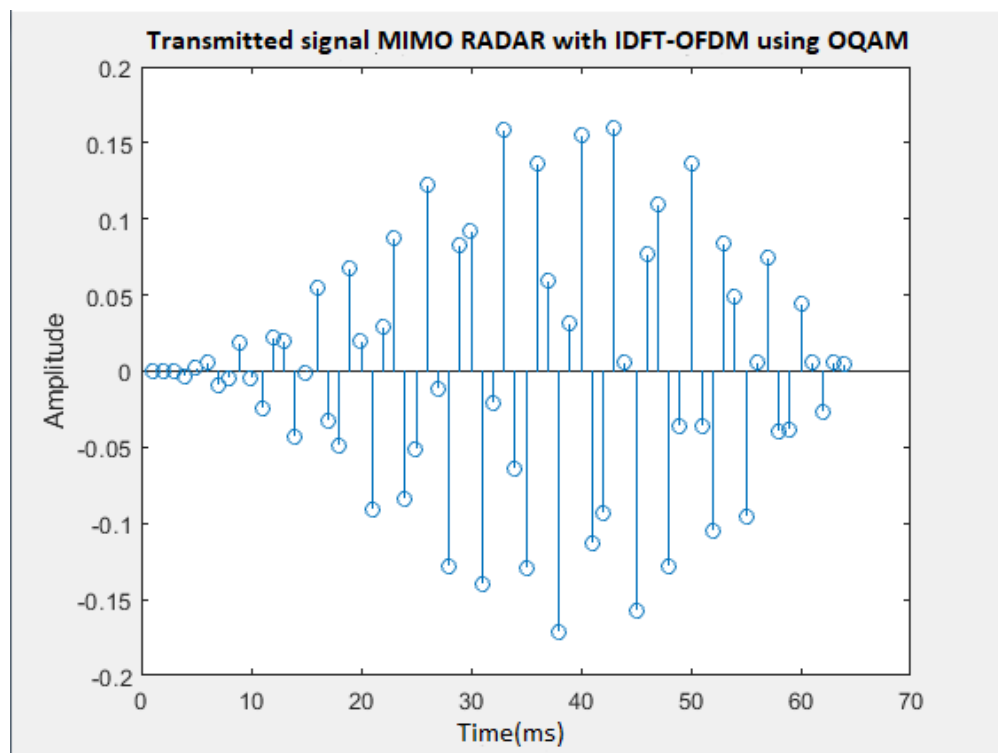
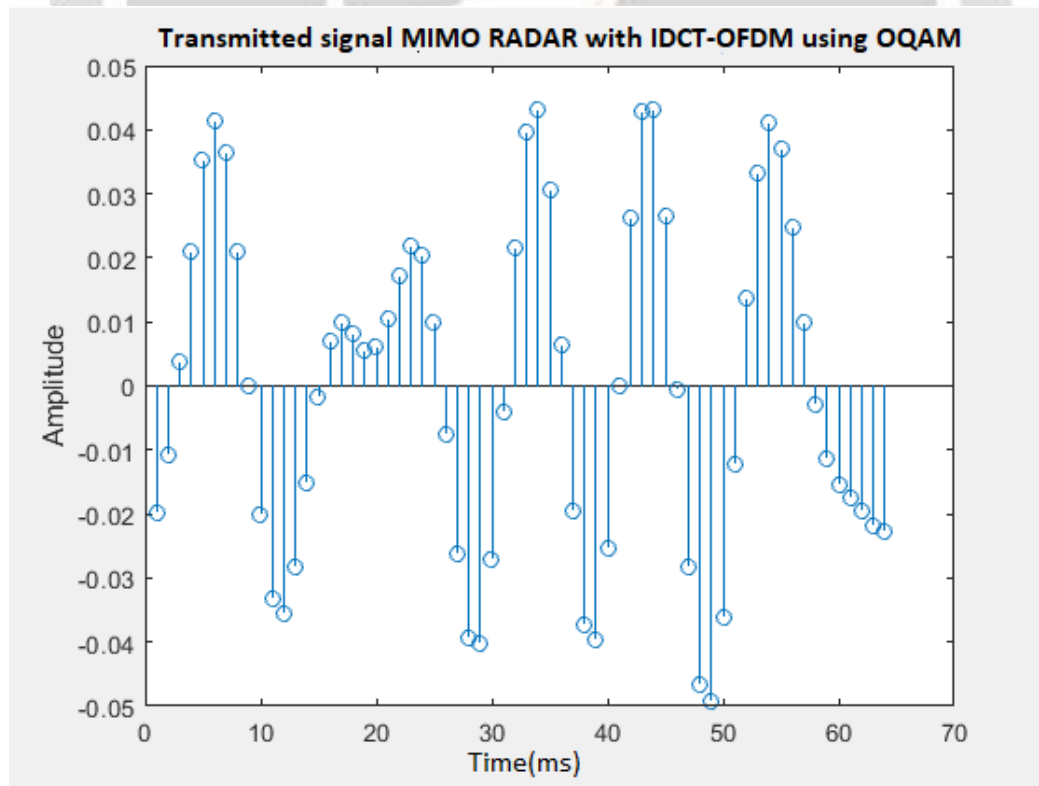**Fig. 10.** *Transmitted signal MIMO RADAR with IDFT-OFDM using OQAM*



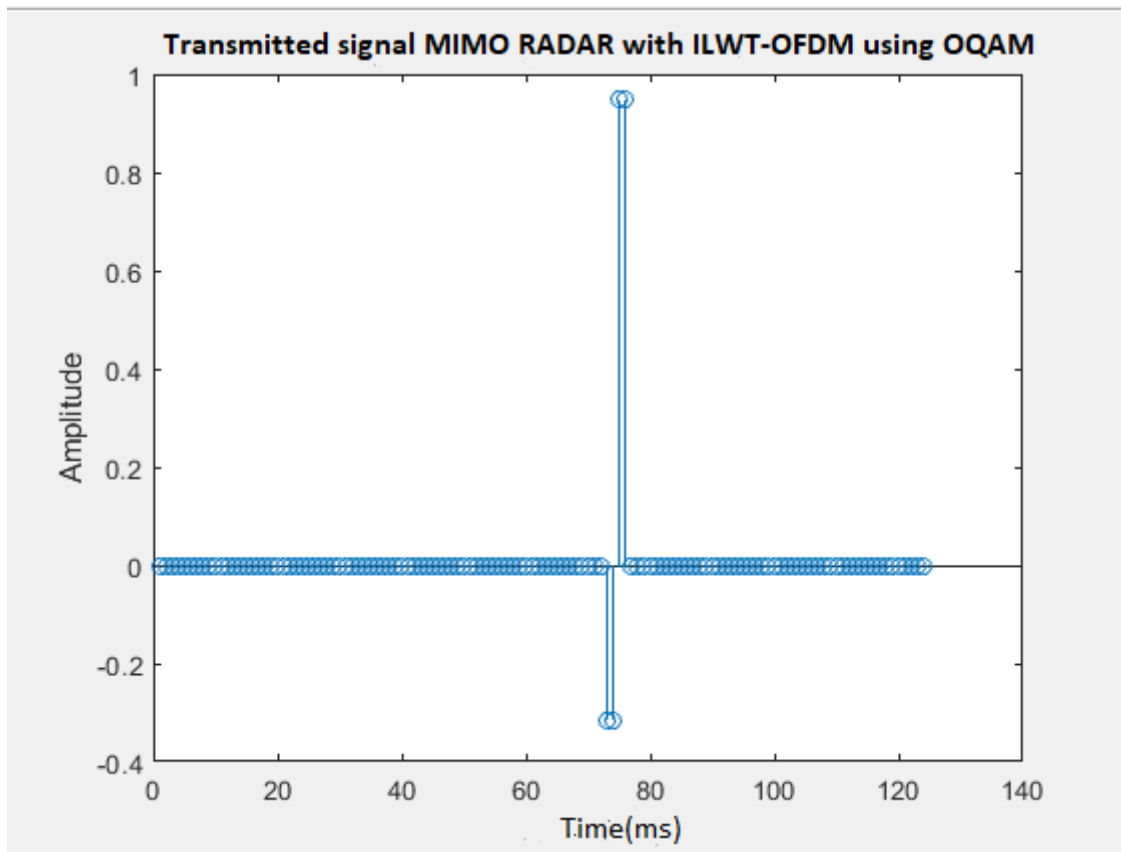**Fig. 11.** *Transmitted signal MIMO RADAR with IDCT-OFDM using OQAM*

**Fig. 12.** *Transmitted signal MIMO RADAR with ILWT-OFDM using OQAM*

### 3.3 PAPR of the multiple transform

As the interpretation of the modulated signal, the Peak Average Power Ratio shows in fig. 13 that ILWT presents a very low PAPR. With the same power of power amplifier, the ILWT-OFDM could achieve more distance than the others. Indeed, also, the ILWT uses a quick computational using biorthognal interpolation which is obtained by just addition and substraction, just like in the equation 25, 28, 32, 34.

The IDFT and IDCT should use exponential forms and need infinite computation of polynom interpolation. So, the ILWT-OFDM also doesn't spend more power than the IDFT-OFDM and IDCT-OFDM.

The first implementation of multi-carrier modulation using IDF, IDCT, has a very bad PAPR. Some techniques like PAPR reduction and pre-distorsion could improve this problem of power consumption. In this article, we can see that ILWT-OFDM doesn't need another block of PAPR reduction because the wavelet transform reduces this by default.So, with the same power, the ILWT-OFDM could achieve, longer range than IDC-OFDM and IDFT-OFDM which is very useful in the RADAR MIMO.

After the simulation, the ILWT is the best option for PAPR reduction using OFDM modulation instead of IDCT and IDFT when we do 8 tests. But, the technique has also some disadvantages, like the power spectrum not being used more and the bit error ratio being more larger.
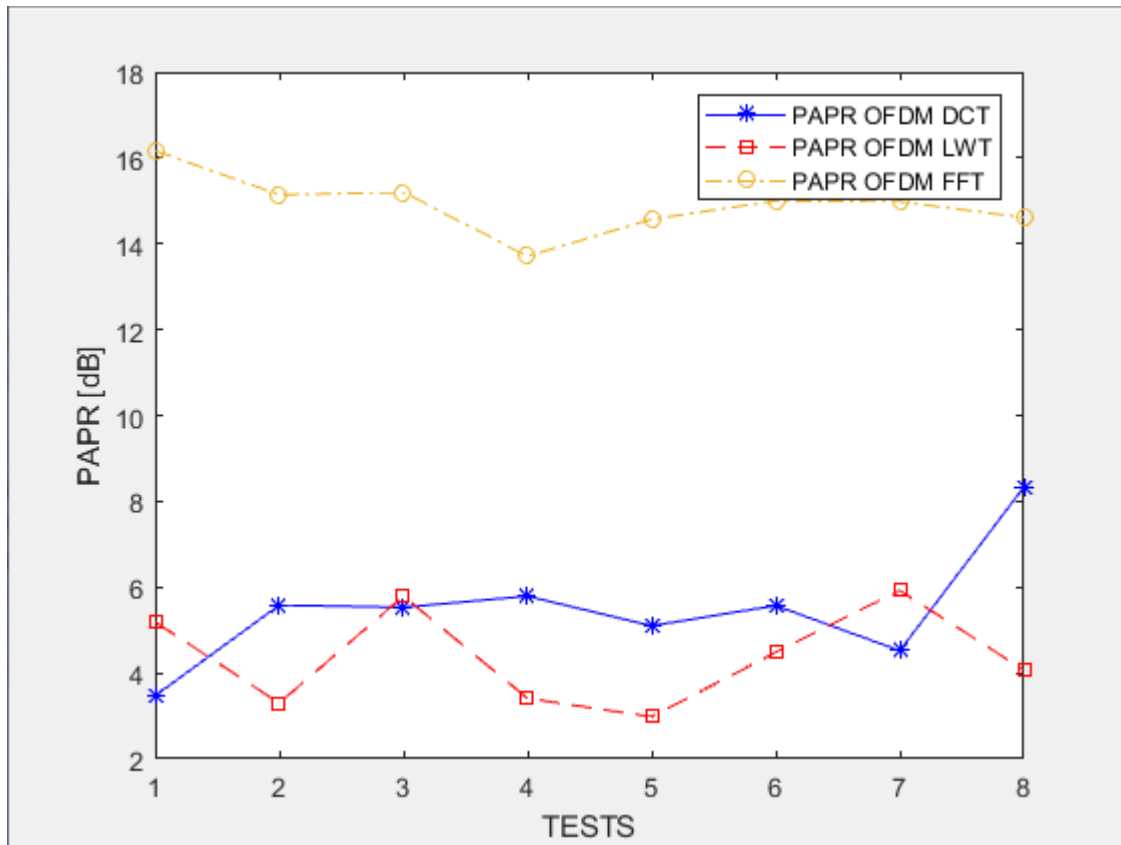
**Fig. 13.** *Evaluation of PAPR using Multiple Transform (DFT, DCT, LWT)*

### 3.4 BER of the multiple transform

The fig.5 and fig. 6 are a complete transmission chain using OFDM with multiple transforms.

So, it's possible to compare the signal to be sent and the signal received and compare the number of bit errors. This number of bit errors is divided by the total number of bits by having a Bit Error Ratio (BER). On the fig. 12 and 13, the BER of OFDM-FFT is a bit similar to OFDM-LWT and the DCT is not more suitable for OFDM modulation.
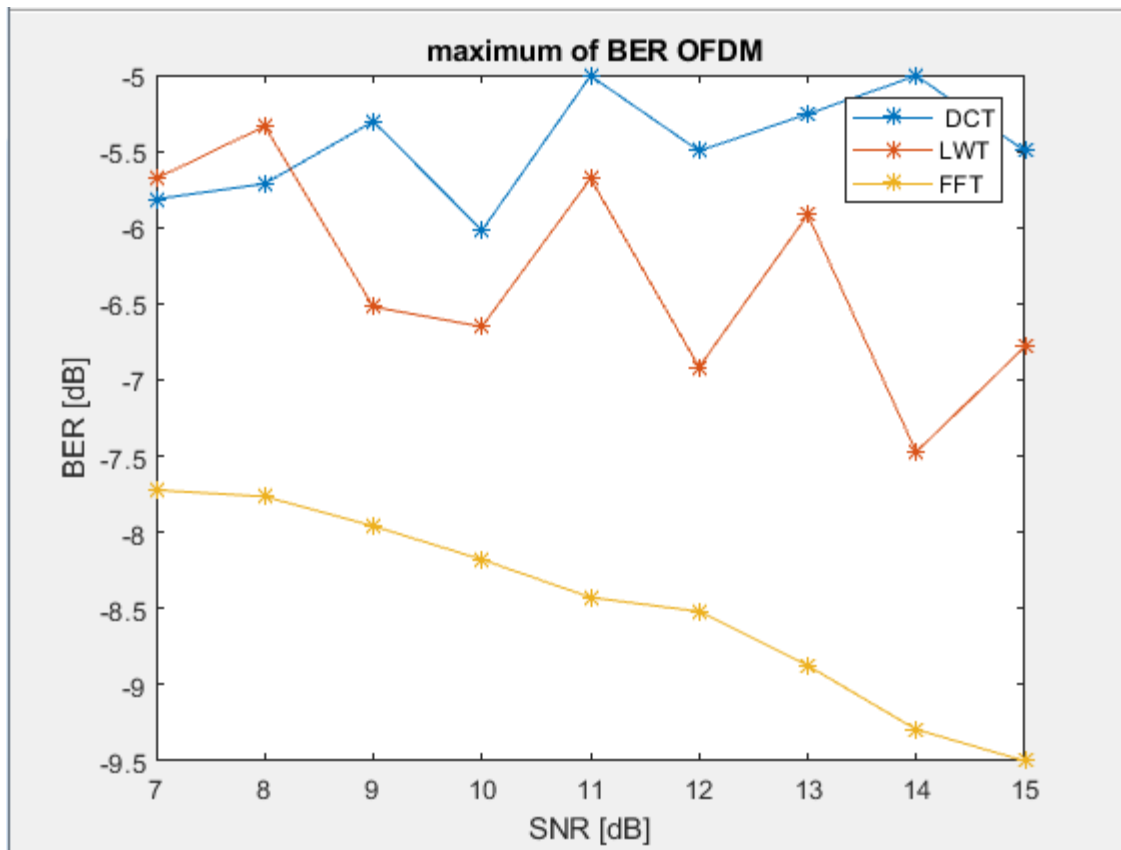
**Fig. 14.** *Evaluation of BER using Multiple Transform (DFT, DCT, LWT)*

## 4. CONCLUSIONS

As conclusion, OFDM-ILWT gives a good power consumption with MIMO-RADAR. The wavelet transform is very quick and has a less PAPR. The OFDM-IDCT is the second choice but it's not have a quick time processing. For having high data rate, the OFDM-ILWT should use a good code corrector error to resolve the problem about Bit Error Ratio (BER). This proposition is not so useful on RADAR MIMO due less data rate transmitted on it.

## 5. REFERENCES

[1]. Zhou, Zhenlei, Lin, Bangjiang, Tang, Xuan, Chaudhary, Sushank, Lin, Chun, "Performance comparison of DFT-OFDM, DCT-OFDM, and DWT-OFDM for visible light communications", spie. Journal, International Conference on Optical Communications and Networks, 2018, Zuhai China.

[2]. Javaid A. Sheikh, Farhana Mustafa, Arshid Iqbal "Resource Allocation of Power in FBMC based 5G Networks using Fuzzy Rule Base System and Wavelet Transform", International Journal of Advanced Research in Science and Engineering (IJARSE), march 2018.

[3]. Zainab Hdeib Al-Shably, Zahir M. Hussain, "Performance of FFT-OFDM versus DWT-OFDM under Compressive Sensing", Journal of Physics: Conference Series, 2021

[4]. Khaizuran Abdullah, Zahir M. Hussain, "Studies on DWT-OFDM and FFT-OFDM Systems", International Conference on Communication, Computer and Power (ICCCP 2009)

[5]. Elif Büşra Tuna, Yusuf İslam Tek, Ali Ozen, "A Novel Approach based on Lifting Wavelet Transform for MIMO-OFDM Systems", Research square 2021

[6]. Sheela M. S., Sukera T. P., Arjun K. R., "Comparaison of FFT-OFDM and DWT-OFDM System in Digital Communication", International Journal of Engineering Research and Technology, IJERT 2018

[7]. Meryem Maras, Elif Nur Ayvaz, Meltem Gömeç, Asuman Sava̧scıhabes, Ali Özen, "A Novel GFDM Waveform Design Based on Cascaded WHT-LWT Transform for the Beyond 5G Wireless Communications", MDPI 2021

[8]. Shanlin wei, Hui li, Wenjie Zhang, Wei Cheng, "A comprehensive performance evaluation of Universal Filtered Mutli-Carrier Technique"

[9].    Zahraa Abdel Hamid, Fathl E. Abd El Samie, ″FFT/DWT/DCT OFDM channel estimation using EM algorithm in the presence of chaotic interleaving″, IEEE 2012

[10].    Mitali Sahu, Meha Shrivastava, Abhishek Agwekar, ″Review of PAPR reduction for MIMO-OFDM Radar with DWT and DCT Multiple Contrainsts″, International Journal of Engineering Research and Technology, IJERT 2019.

[11].    B.Prasanna Lakshmi, K.Govinda Rajulu, ″DWT based barcode modulation for efficient and secure data transmission through DPSK-OFDM″International Research Journal of Engineering and Technology, IRJET, 2017

[12].    Enggar Fransiska DW, Octarina Nur Samijayan, J Suci Rahmatia, ″Design and Performance Investigation of Discrete Wavelet Transform (DWT) Based OFDM using 4-PAM for Indoor VLC System″, International Conference on Information and Communication Technology, ICoICT 2019

[13].    Ch.Gangadhar, Md. Habibulla, ″Spectral Efficiency Enhancement Through Wavelet Transform Filter Bank for Future Mobile Communications″, International Journal of Innovative Technology and Exploring Engineering, IJITEE 2019

[14].    Elif Nur Ayvaz, Meryem Maras, Meltem G¨omec, Asuman Savas¸cıhabes, Ali  Ozen, ″A Novel Concatenated LWT and WHT Based UFMC Waveform Design for the Next Generation Wireless Communication Systems″ IEEJ TRANSACTIONS ON ELECTRICAL AND ELECTRONIC ENGINEERING, 2021

[15].    Engin ÖKSÜZ, Ahmet ALTUN, Büşra ÜLGERLİ, Gökay YÜCEL, Ali ÖZEN, ″A Comparative Performance Analyses of FFT Based OFDM and DWT Based OFDM Systems″, journal of new result in science, JNRS 2016

[16].    Simmi Garg, Anuj Kumar Sharma, Anand Kumar Tyagi, ″Performance Comparison of Proposed Scheme Coded DWT-OFDM System with that of Conventional OFDM″, Journal of Unversity of Shanghai for Science and Technology, 2020

[17].    Manjunatha K, Reshma M, ″Comparative Study on DWT-OFDM and FFT-OFDM Simulation Using Matlab Simulink″, International Journal of Engineering Trends and Technology, IJETT, 2017

[18].    Wim Sweldens, ″The Lifting Scheme: A New Philosophy in Biorthogonal Wavelet Constructions″, Department of Computer Science